CARPATHIAN J. MATH.
20 (2004), No. 2, 251 - 259

From Nano-Peapods through DWNTs to Elongated Tori

CSABA L. NAGY and MIRCEA V. DIUDEA

ABSTRACT. The encapsulation of fullerene cages inside single-walled nanotubes SWNT can be performed very efficiently in both vapor phase and in solution. In the inner space of SWNT, zero dimensional molecules, like C_{60}, are ordered in one-dimensional arrays. Such structures are called nanopeapods. Annealing peapods over 800^{o}C, results in double-walled carbon nanotubes DWNT. We propose that controlled irradiation at the tip of nano-peapods could initiate the fusion between the inner and parent nanotube, resulting a torus.

1. INTRODUCTION

The merging process between carbon nanostructures, induced by thermal annealing or electron beam irradiation, is a way to the synthesis of more complex structures: double-walled nanotubes DWNT can be synthesized by merging fullerene molecules into a nanotube to form nanopeapod systems [1]; two nanotubes coalesce into a diameter-doubled one [2,3]; initially crossed nanotubes can form "Y" and "T" shaped junctions [4], etc.

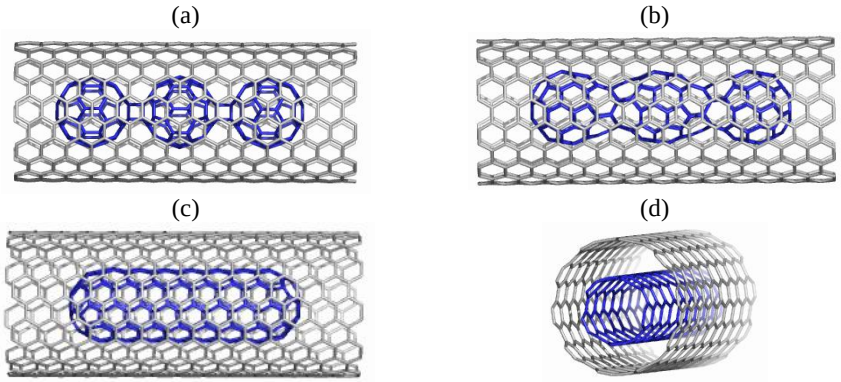

Figure 1. From the [2+2] cycloadduct of C_{60}, to peapods and double walled nanotube DWNT.

Recently coalescence was observed experimentally during thermal annealing/irradiating of nano-peapods [5,6]. Since fullerene molecules are arranged in a one-dimensional array inside the nanotube, fusion can occur only between neighbouring molecules. Depending on the initial orientation of fullerene cages the shape of the intermediates may vary, however the process always finalize with the formation of a new

Received: 26.09.2004; In revised form: 17.01.2004
2000 *Mathematics Subject Classification.* 92E10
Key words and phrases. *peapods, torus, fullerene, DWNT, coalescence*

nanotube. The diameter of the inner tube at first corresponds with that of the initial fullerene, and increase up to the van der Waals distance to the external parent tube [1]. Figure 1 illustrates this multi-step process in case of the coalescence of C_{60} molecules inside an armchair nanotube. Note that the initial step is the formation of [2+2] cycloadducts also occurring in the bulk polymerization process of fullerenes [7].

2. DOUBLE WALLED TORUS - DWT

The following section presents our construction method of tori from armchair DWNTs, and calculation results on series of tori. Note that similar tori have been previously proposed by several authors [8-11], but no relation with peapods, coalescence and DWNT was suggested. Also note that hemitori, resembling with our DWTs, have been observed by TEM and inferred in multi walled nanotube growth [12].

2.1. CONSTRUCTION, TOPOLOGY

It was above discussed that coalescence is also induced by electron beam irradiation, when vacancies and dangling bonds appear in the carbon lattice and energy reduction is achieved by elimination of such defects. Field emission electron guns are available, which permit the controlled irradiation of a small region on the nanometer scale. The dangling bonds, generated by irradiation, could stabilize themselves by forming new bonds between the two interlaced tubular units. This would result in formation of an elongated torus, named hereafter "distinct-walled torus" DWT. Various types of DWTs, built up from only armchair nanotubes, are further presented.

The inner tube is shown in Figure 2 by the top hexagons. Breaking of the boldface bonds results in two dangling bonds. To remake the valence of three, each dangling bond has to connect with two carbon atoms from the outer tube (see dotted bonds in Figure 2). That is why twice as much carbon atoms in a row in the outer tube are needed. Of course, the growth of the inner tube depends on the outer tube diameter.

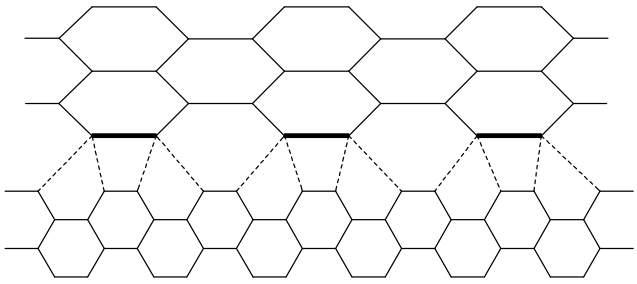

Figure 2. Joining scheme of the two distinct tubes in DWT formation.

The junction between the two tubes consists of alternating pentagon/octagon/ pentagon *pop* triplets, which ensure the complementary curvature and stability of the structure. The elimination of octagons is possible by the Stone-Wales [13] rotation of the bonds connecting the two vicinal pentagons (see Figure 3, bond in boldface). However, the pentagon-heptagon *PH* containing junction appears more strained, after optimization, as shown by increased H_f values (Table 1). It is easily seen (Figure 2) that both these junction coverings provide a PCS. Namely, the non-hexagonal faces are bounded only by single bonds, while the double bonds lye in the benzenoid hexagons.

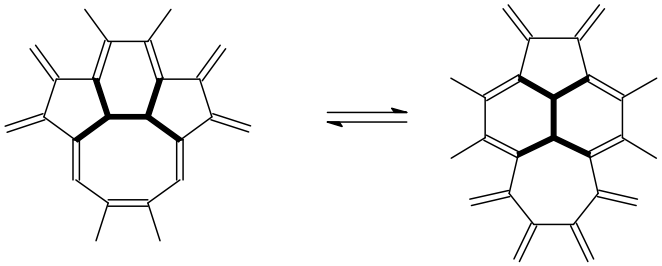

Figure 3. Transformation of the junction between the inner and outer tube of a DWT by Stone-Wales rotation of the boldface bond.

Considering an armchair nanotube with even or odd number of atom rows, the combination of different nanotubes leads to four distinct classes of DWTs, which resembles in their point group symmetry. The torus will have a horizontal plane of symmetry only in case when both tubes have an even number of rows. Figure 4 presents the repeat units of these tori. By copying the lines in boldface for $l_e / l_i = 0, 1, 2 \ldots$ the tube length increases. In case $l_e / l_i = 0$, the smallest possible torus, having abutting pentagons, is obtained.

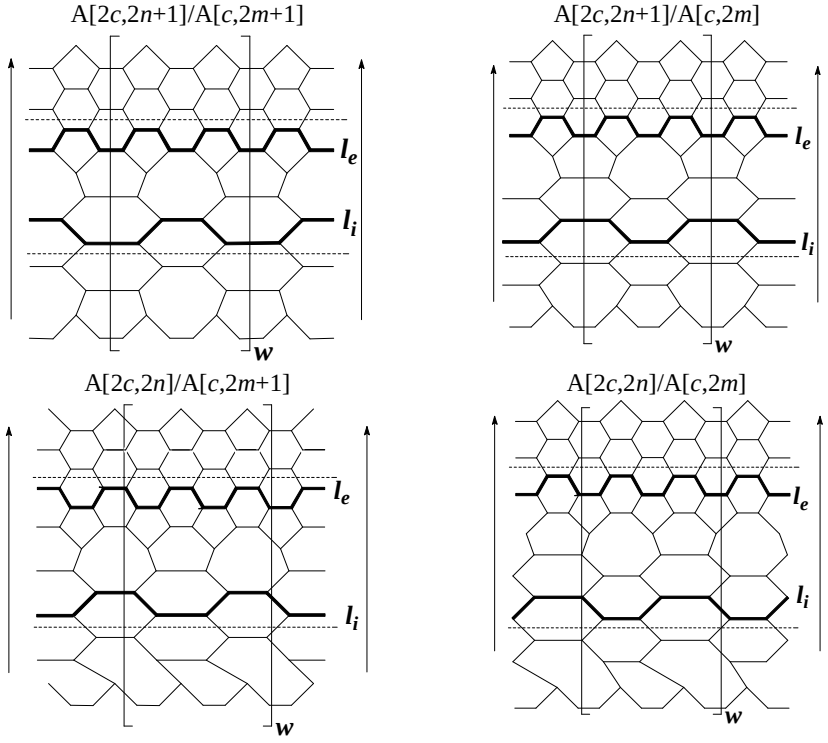

Figure 4. Units of the four *POP*-DWT types in geodesic projection.

The torus width w can be increased by adding more repeat units (in brackets). Although it is possible to construct a torus from one unit, the strain at the apex is reduced starting from $w \geq 4$. The name of these DWTs includes the specification of the two tubes. For example, A[2c,2n+1] corresponds to the outer tube with 2c atoms in a row and odd number of rows (2n+1) in length, while the inner tube A[c,2m+1] has half as many atoms in a row and again an odd number of rows (2m+1) in length. The length of two tubes can be either equal, when $n = m$, or different (Figure 4a).

2.1.1. POP-DWT

Since from the fusion of C_{60} results the A[10,m] nanotube, most of the calculations were performed on the A[20,n]/A[10,m] tori. Tori with larger tube diameter have also been modeled. Figure 5 presents tori with four and six repeat units.

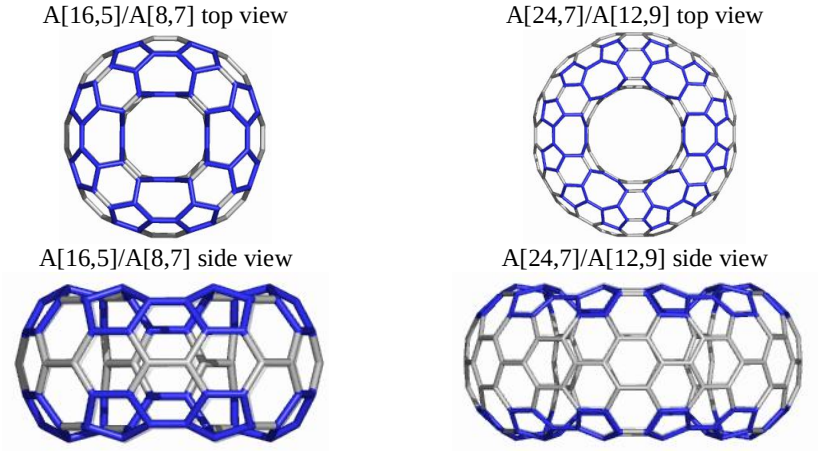

Figure 5. *POP*-DWTs with four/six repeat units.

2.1.2. PH-DWT

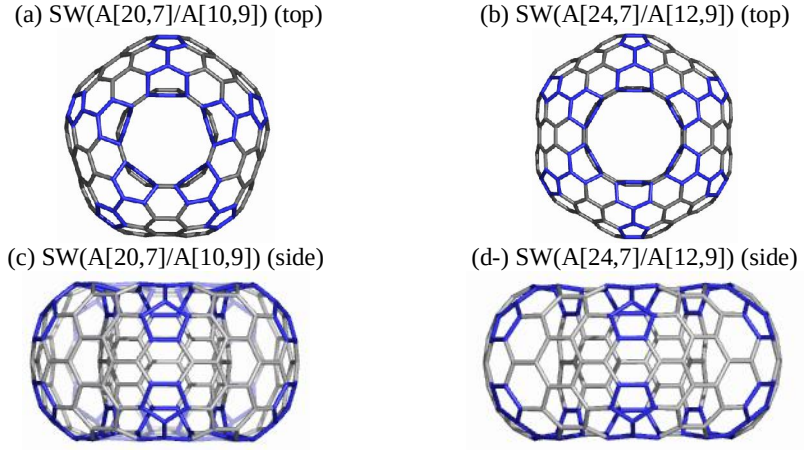

Figure 6. *PH*-DWTs resulted by the SW rotation of bonds joining two pentagons.

Such tori results by the Stone-Wales transformation of the junction zone as presented in Figure 2, changing the triple *POP* to the *PH* pair. Figure 6 presents two structures resulted by such a transformation.

2.1.3. PERFECT CLAR TORI

A molecule is more aromatic (eventually more stable) if it has a perfect Clar structure PCS [14,15]. In DWT, the apex junction of the two tubes looks as shown in Figure 2 (with no double bonds in the odd-fold cycles) and is suitable for a PCS. The criterion for PCS realization refers only to the polyhex tubular zone; for armchair A[*c*,*n*] nanotubes, it is:

POP-DWTs: A[2*c*,3(*n*+1)+1]/A[*c*,3(*m*+1)-1]
PH-DWTs: A[2*c*,3(*n*+2)]/A[*c*,3(*m*+2)]

In the above formulas, 2*c*/*c* represents the number of atoms in the outer/inner tube section, while *n*/*m* denotes the length of the outer/inner tube.

(a) *RLe*(A[20,7]/A[10,8]) (b) *RLe*(SW(A[20,9]/A[10,9]))

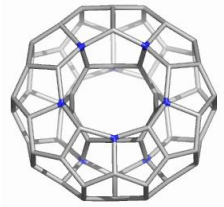

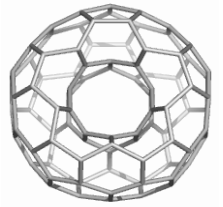

(c) A[20,7]/A[10,8] (d) SW(A[20,9]/A[10,9])

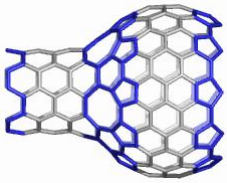

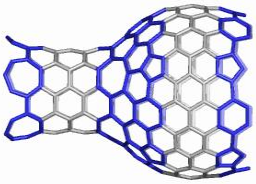

(e) PCS of A[20,7]/A[10,8] (f) PCS of SW(A[20,9]/A[10,9])

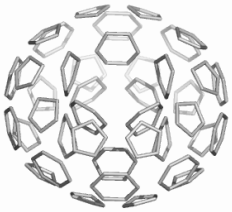

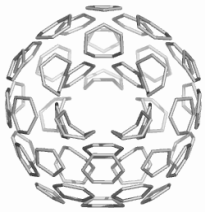

Figure 7. *Retro-Leapfrog* (a, b); PCS junctions (c, d) and Perfect Clar Structure DWTs (e, f).

A PCS object results by the *Leapfrog Le* operation on maps [16]: $Le(M) = Du(P_3(M))$. Keeping in mind that dual of dual returns the original map, the *Retro-Leapfrog RLe*, leading to the parent torus, can be written as follows: $Du(Le(M)) = P_3(M)$ and $RLe(M) = P_{-3}(M)$, with P_{-3} being the *retro*-operation of stellation P_3.

The parent of a *POP*-DWT has the corresponding vertices of valence four (Figure 7a, in dark). The SW pair *PH*-DWT has an all trivalent parent map, as illustrated in Figure 7b. The corresponding junction zones are detailed in Figure 7c,d. The PCS of A[20,7]/A[10,8] and SW(A[20,9]/A[10,9]) tori are given in Figure 7e,f.

3. Results And Discussion

The topology of the zone joining the two tubes of a DWT influences both the strain and heat of formation. Keeping constant one tube and varying the length of the other one enables construction of a series of tori. Semiempirical calculations are presented in Table 1 and Figures 8-9. The minimal energy corresponds to the most relaxed structure. When there is a notable difference between the tubes length, the energy increases due to hexagons forced to lie at the apex. At extreme low/high values of *m*, the structure could not be optimized anymore. Figure 8 shows the energy curve for a series of *POP*-DWTs, where the inner tube length varied in the range *m* = 4,5... The structure with lowest energy was found A[20,5]/A[10,8].

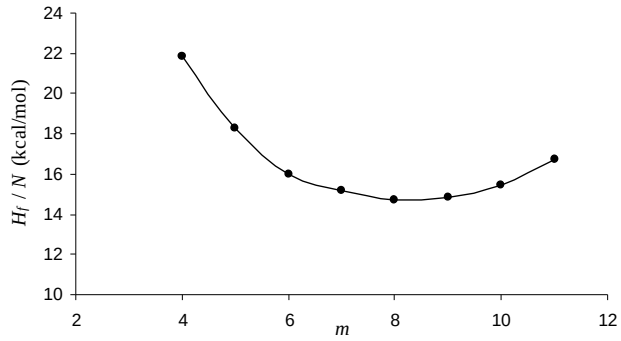

Figure 8. Heat of formation values for the series A[20,5]/A[10,*m*] *m* = 4,5…11. of *POP*-DWTs.

The plot in Figure 9 shows a series of *POP*-DWTs with the inner tube length maintained constant.

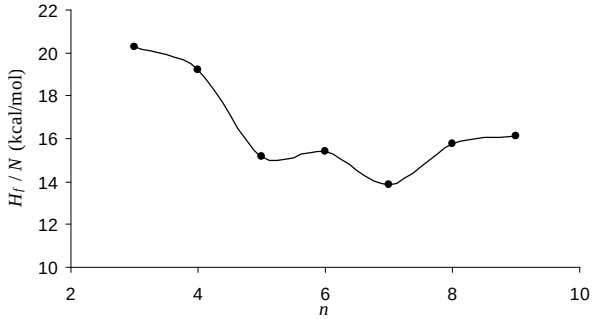

Figure 9. Heat of formation values for the series A[20,*n*]/A[10,7] *n* = 3,5…9 of *POP*-DWTs.

If the length of both tubes was increased by the same number of rows, the junction zone shoved an almost constant strain. The global strain energy decreases as the tube length increases (Figure 10).

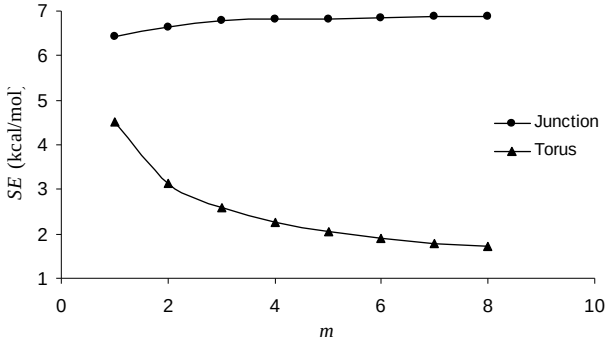

Figure 10. Strain energy for the series A[20,*n*]/A[10,*m*], n = 7, 13,…49; m = 11, 17, …53 of *POP*-DWTs.

We limited here to only A[20,*n*]/A[10,*m*] tori, because these DWTs could result in the coalescence of fullerene molecules. DWTs with larger central hollow have also been modeled, in studying the influence of the primary tube diameter on the structure stability. In this respect, a series of tori was constructed: the length was kept unchanged but the number of repeat units was varied. The tori consisting of one to three repeat units were very strained, they could not be optimized.

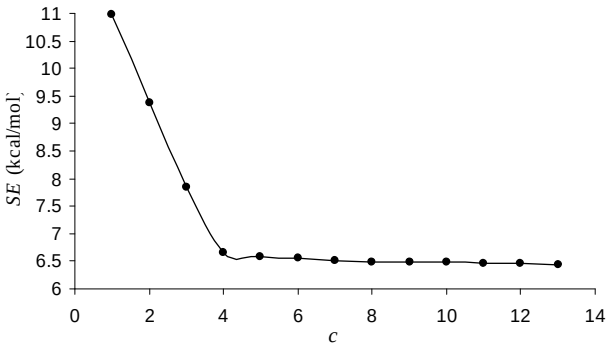

Figure 11. Strain energy for the series A[2*c*,7]/A[*c*,5], c = 4, 6, …30 of *POP*-DWTs.

Table 1. Variation of stability in series of POP- and PH-DWT.

Name	*N*	Sym	*POP-DWT*		*PH-DWT*	
			H_f/N (kcal/mol)	Gap (eV)	H_f/N (kcal/mol)	Gap (eV)
A[20,5]/A[10,7]	170	D_{5h}	15.159	5.031	18.202	4.815
A[20,7]/A[10,9]	230	D_{5h}	12.122	5.685	14.311	4.547
A[20,9]/A[10,11]	290	D_{5h}	10.827	4.218	12.249	5.078
A[20,5]/A[10,6])	160	D_{5d}	15.978	5.134	17.032	4.719
A[20,7]/A[10,8]	220	D_{5d}	12.678	5.589	13.731	4.584
A[20,9]/A[10,10]	280	D_{5d}	11.376	4.092	11.870	4.825
A[20,4]/A[10,6]	140	D_5	20.306	5.967	20.306	5.967
A[20,6]/A[10,8]	200	D_5	14.408	4.988	14.408	4.988
A[20,8]/A[10,10]	260	D_5	12.319	4.051	12.319	4.051

As above mentioned, DWTs with a *PH* junction are less stable than their corresponding SW *POP* pair. It is generally true, excepting the case they have a perfect Clar structure PCS; both the kinetic and thermodynamic stability of a PCS *PH*-DWT is higher than its PCS *POP*-DWT pair. Table 2 presents semiempirical data performed on PCS DWTs.

Table 2. Semiempirical data for PCS DWT.

Name	*N*	H_f / *N* (kcal/mol)	GAP (eV)	Sym	Junction type
A[20,7]/A[10,8]	220	12.678	5.589	D_{5d}	*POP*
A[20,7]/A[10,11]	250	12.274	4.518	D_{5h}	*POP*
A[20,9]/A[10,9]*	270	12.441	3.725	D_{5h}	*POP*
SW(A[20,9]/A[10,9])	270	12.051	4.266	D_{5h}	*PH*

*This torus doesn't have a PCS, it's stability must be compared to the SW pair which has a PCS.

4. CONCLUSIONS

The finally resulted double-walled nanotubes DWNTs could be precursors of distinct-walled tori DWTs, with the apex zones decorated by non-hexagonal faces. Semiempirical calculations proved that such tori are far more stable than the classical polyhex ones, at least at small and moderate size.

It was found that DWTs become more relaxed by the increase of the tube length. A supplementary stability is brought by the PCS. We limited here to the armchair achiral nanotubes, but it is also possible to construct tori from chiral nanotubes.

REFERENCES

[1] Bandow, S., Hiraoka, T., Yumura, T., Hirahara, K. and Iijima, S., Chem. Phys. Lett. **384** (2004), 320-325.

[2] Terrones, M., Terrones, H., Banhart, F., Charlier, J-C. and Ajayan, P. M., Science **288** (2000), 1226-1229.

[3] Banhart, F. J. of Electron. Microsc. **27** (2002), 189-194.

[4] Terrones, M., Banhart, F., Grobert, N., Charlier, J.-C., Terrones, H. and Ajayan, P. M., Phys. Rev. Lett. **89** (2002), 075505(1)-(4).

[5] Bandow, S., Takizawa, M., Hirahara, K., Yudasaka, M. and Iijima, S., Chem. Phys. Lett. **337** (2001), 48-54.

[6] Hernández, E., Meunier, V., Smith, B. W., Rurali, R., Terrones, H., Buongiorno Nardelli, M., Terrones, M., Luzzi, D. E. and Charlier, J.-C., Nano Lett. **3** (2003), 1037-1042.

[7] Iwasa, Y., Arima, T., Fleming, R. M., Siegrist, T., Zhou, O., Haddon, R. C., Rothberg, L. J., Lyons, K. B., Carter Jr., H. L., Hebard, A. F., Tycko, R., Dabbagh, G., Krajewski, J. J., Thomas, G. A. and Yagi, T., Science **264** (1994), 1570-1572.

[8] Itoh, S., Ihara, S. and Kitakami, J.-I., Phys. Rev. B **47** (1993), 1703-1704.

[9] Ihara, S., Itoh, S. and Kitakami, J., Phys. Rev. B **47** (1993), 12908-12911.

[10] Itoh, S. and Ihara, S., Phys. Rev. B **49** (1994), 13970-13974.

[11] Itoh, S. and Ihara, S., Phys. Rev. B **48** (1993), 8323-8328.

[12] Endo, M., Takeuchi, K., Kobory, K., Takahashi, K., Kroto, H. W. and Sarkar, A., in *Carbon Nanotubes* (Endo, M., Iijima, S. and Dresselhaus, M. S., Eds.), Pergamon, 1996, pp. 1-9.

[13] Stone, A. J. and Wales, D. J., Chem. Phys. Lett. **128** (1986), 501-503.

[14] Clar, E., *The Aromatic Sextet*, Wiley, New York, 1972.

[15] Clar, E., *Polycyclic Hydrocarbons*, Acad. Press, London, 1964.

[16] Diudea, M. V., John, P. E., Graovac, A., Primorac, M. and Pisanski, T., Croat. Chem. Acta **76** (2003), 153-159.

BABEŞ - BOLYAI UNIVERSITY
FACULTY OF CHEMISTRY AND CHEMICAL ENGINEERING
ARANY JÁNOS 11, 40028, CLUJ,
ROMANIA
E-mail address: diudea@chem.ubbcluj.ro